High-fidelity numerical simulations of hypersonic high-enthalpy flows

Donatella Passiatore
Postdoctoral Fellow, CTR Stanford University

Advanced Modeling & Simulation (AMS) Seminar Series
NASA Ames Research Center, June 1st, 2023



Acknowledgements



Prof. Paola Cinnella

SCIENCES SORBONNE UNIVERSITÉ

∂'Alembert Institut Jean le Rond ∂'Alembert



Prof. Giuseppe Pascazio

Politecnico di Bari

Dipartimento Meccanica Matematica Management



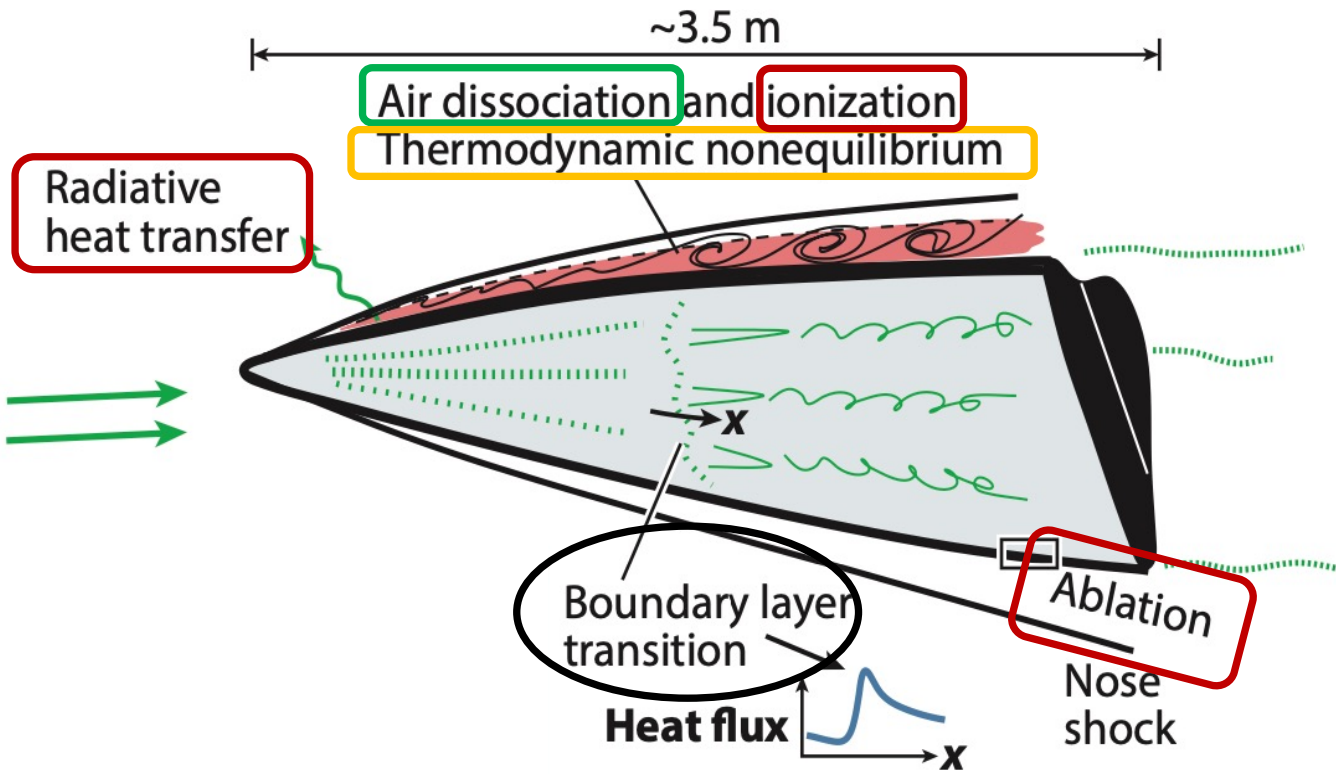
Prof. Luca Sciacovelli

Arts et Métiers Sciences et Technologies

DynFluid Fluid Dynamics Laboratory

Motivation

- High Mach number
- High-enthalpy
- Relatively low altitude



Assessing the interaction between high-enthalpy effects and transition to turbulence/fully turbulence, by means of DNS

State of the art

Boundary layers + chemical reactions:

- Malik and Anderson (1991): Linear stability analysis
- Marxen et al. (2013, 2014): First stages of transition
- Duan and Martin (2011): Temporally evolving boundary layer
- Di Renzo and Urzay (2021), Passiatore et al. (2021), Li et al. (2022): Spatially evolving boundary layer
- Volpiani (2021): Shock-wave boundary layer interaction

+ vibrational excitation:

- Knisely et al. (2019): Linear stability analysis
- Passiatore et al. (2022): Spatially evolving boundary layer
- Passiatore et al. (2023): Shock-wave boundary layer interaction

+ ionization + gas surface interaction and/or ablation + radiation:

- Fundamental studies ..

Modeling and numerical approach

- Multi-component Navier-Stokes equations. Additional equations for species in the mixture and vibrational energy
- Variable heat capacities. Thermally-perfect equation of state
- Multicomponent molar diffusion
- Transport properties as a function of temperature and species mass fractions
- 5-species (N_2, O_2, NO, O and N) with dissociation chemistry and thermal non-equilibrium (Park's 2T model)

Modeling and numerical approach

High-order numerical schemes for high-enthalpy hypersonic turbulent flows:

- Hybrid-schemes: Skew-Symmetric + ENO-type schemes (Di Renzo and Urzay 2020)
- Dispersion Relation Preserving schemes (Volpiani 2021)
- High-order WENO schemes (Li et al. 2022)
- **High-order central schemes + nonlinear artificial dissipation** (Sciacovelli et al. 2021)

Central part
High-order dissipation
Low-order dissipation (shock-capturing)

$$\mathcal{F}_{j+\frac{1}{2}} = \left[\left(I - \sum_{p=0}^{P} a_p \delta^{2+2p} \right) \mu f - \rho(A) \left(\varepsilon_2 \delta w + \varepsilon_{2(P+2)} \delta^{2P+3} w \right) \right]_{j+\frac{1}{2}} \quad \text{with} \quad \begin{cases} \varepsilon_{2_{j+\frac{1}{2}}} = k_2 \max(\varphi_j, \varphi_{j+1}) \\ \varepsilon_{2(P+2)_{j+\frac{1}{2}}} = \max(0, k_{2(P+2)} - k_\varepsilon \varepsilon_{2_{j+\frac{1}{2}}}) \end{cases}$$

Cases setup

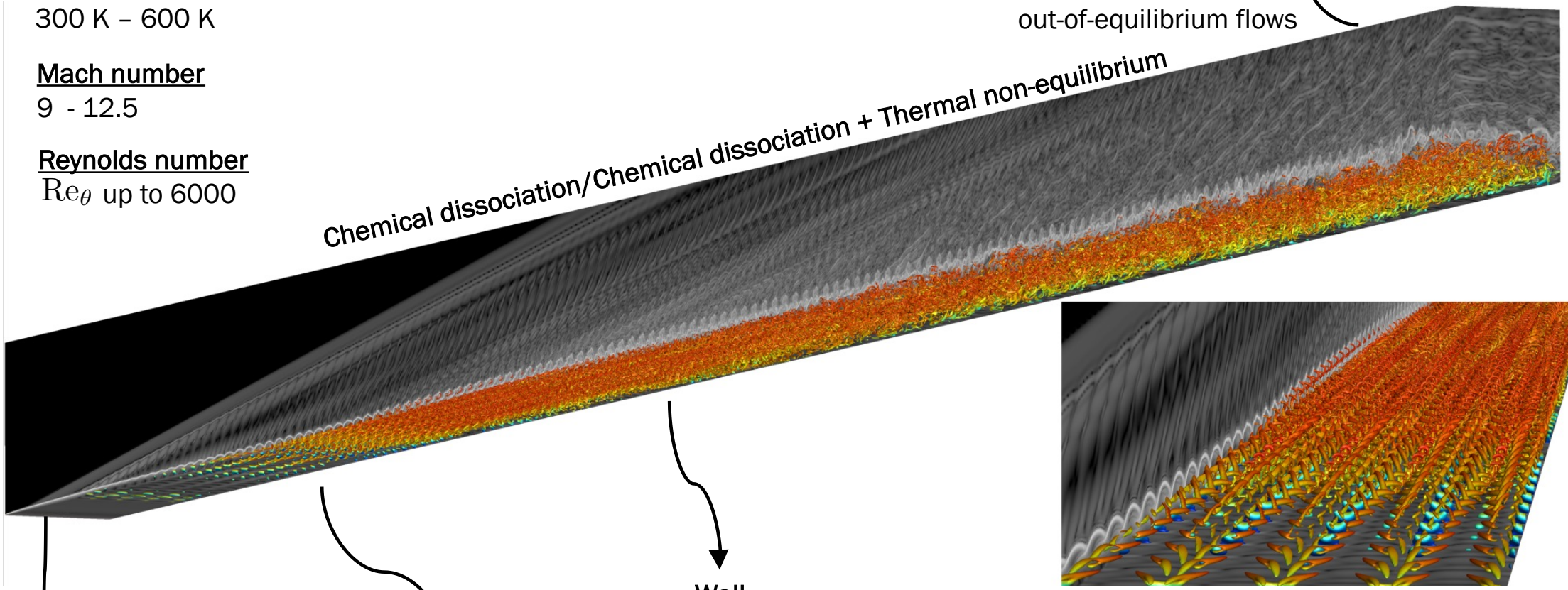
CNE*Adia* *M=10*
TCNE*Cool* *M=12.5*

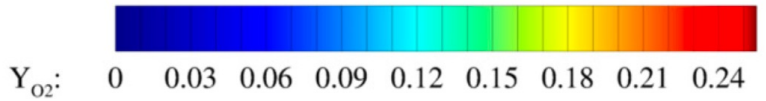
Freestream temperature
300 K – 600 K

Mach number
9 - 12.5

Reynolds number
Re_θ up to 6000

NSCBC
Characteristic BC extended to multi-component thermochemical out-of-equilibrium flows



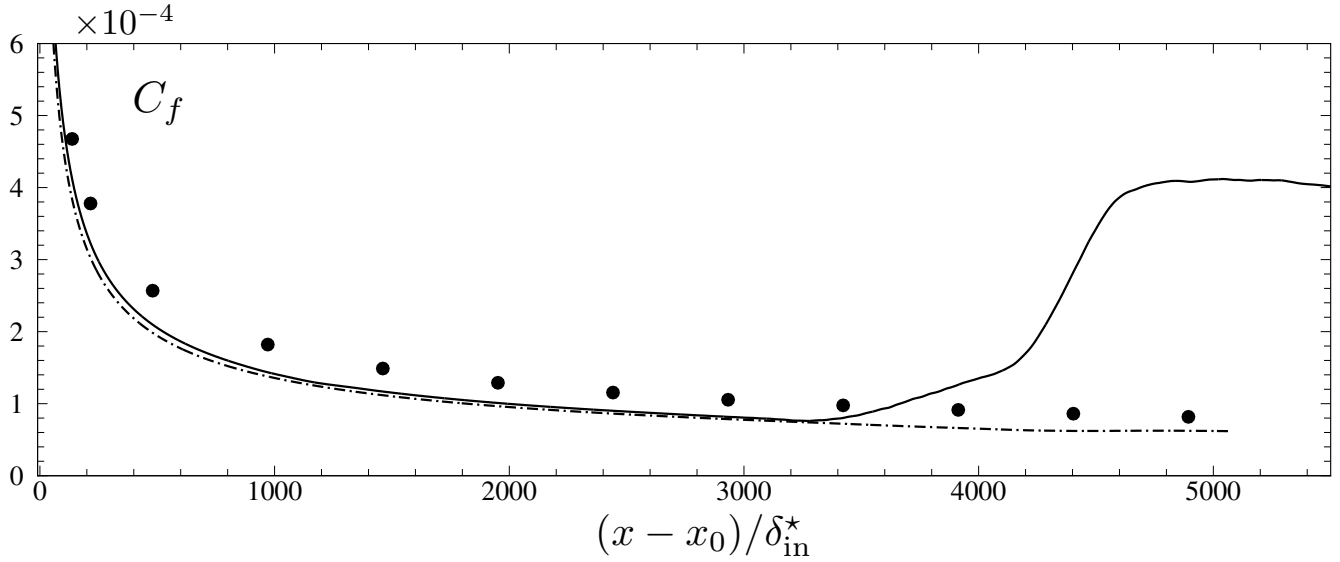


Inflow
Locally self-similar solution

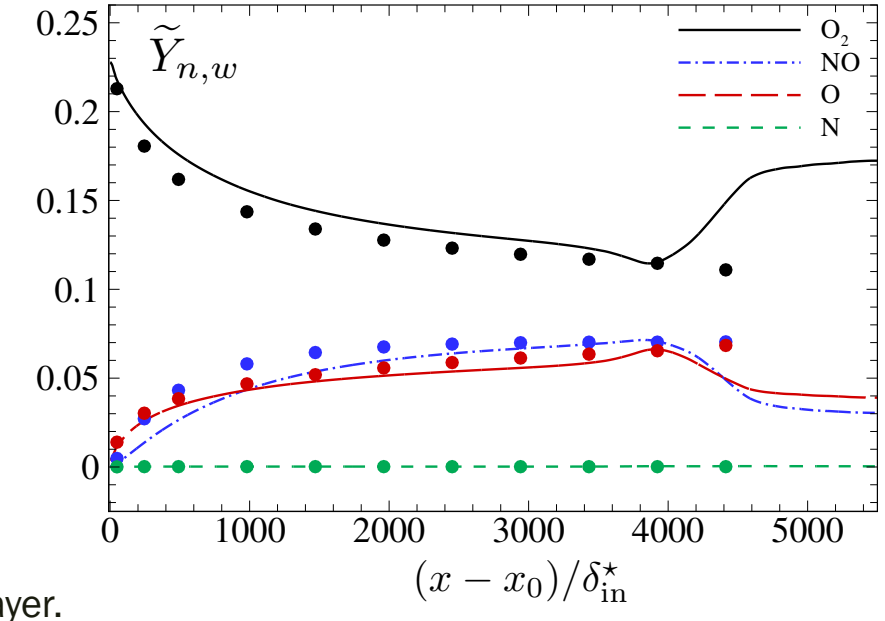
Transition
Modal (suction and blowing)

Wall
Non-catalytic
Thermal equilibrium
Adiabatic/isothermal

Transition & chemistry

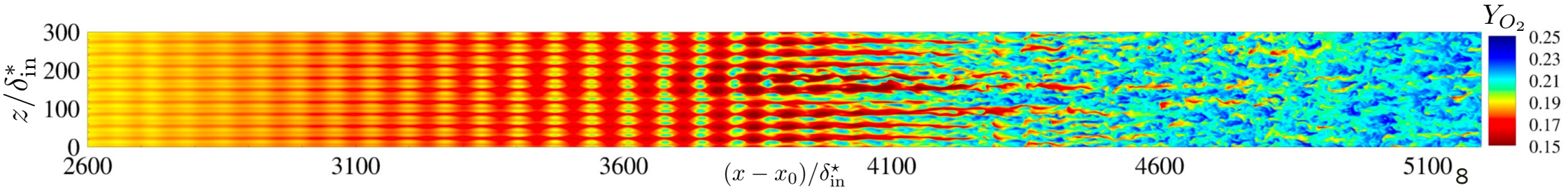


- Locally self-similar solution



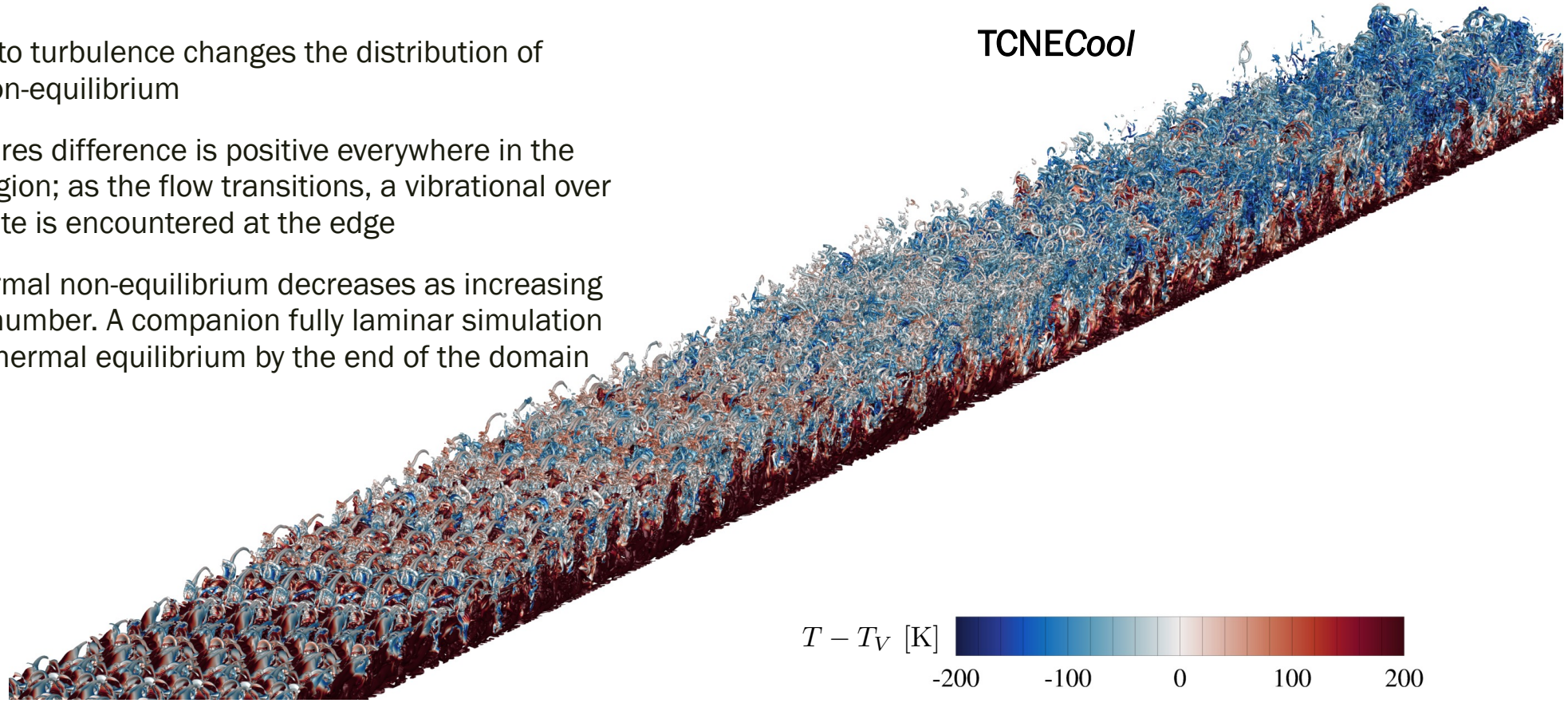
- Species transport equation is in a locally self similar laminar boundary layer. The air mixture is increasingly more dissociated as it flows along the flat plate
- Occurrence of turbulence reduces chemical dissociation of the mixture. Chemical dissociation is slower than the turbulent characteristic time scale

CNE*Adia*

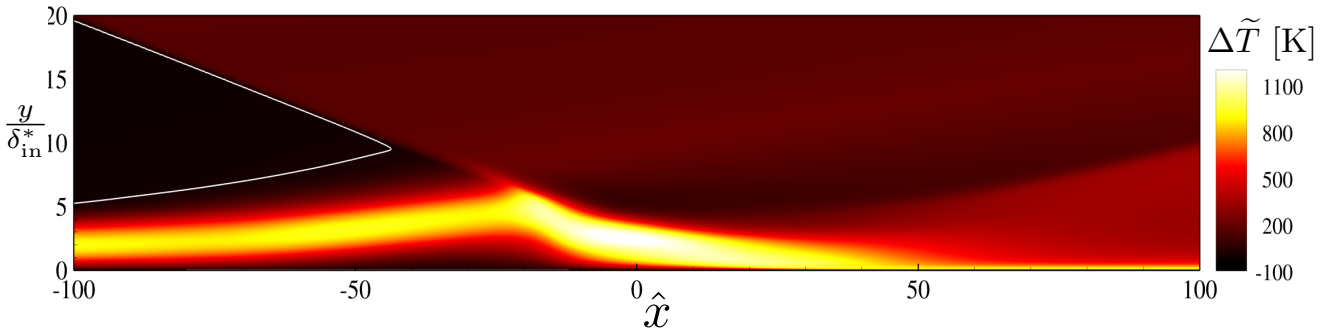


Transition & thermal excitation (I)

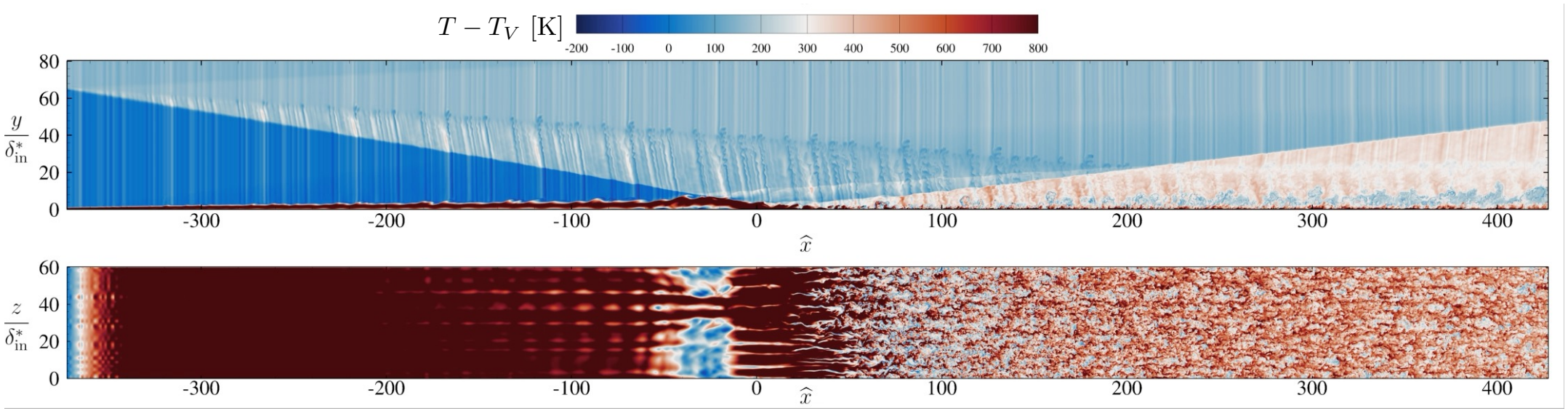
- Transition to turbulence changes the distribution of thermal non-equilibrium
- Temperatures difference is positive everywhere in the laminar region; as the flow transitions, a vibrational over excited state is encountered at the edge
- **NOTE:** thermal non-equilibrium decreases as increasing Reynolds number. A companion fully laminar simulation presents thermal equilibrium by the end of the domain



Transition & thermal excitation (II)

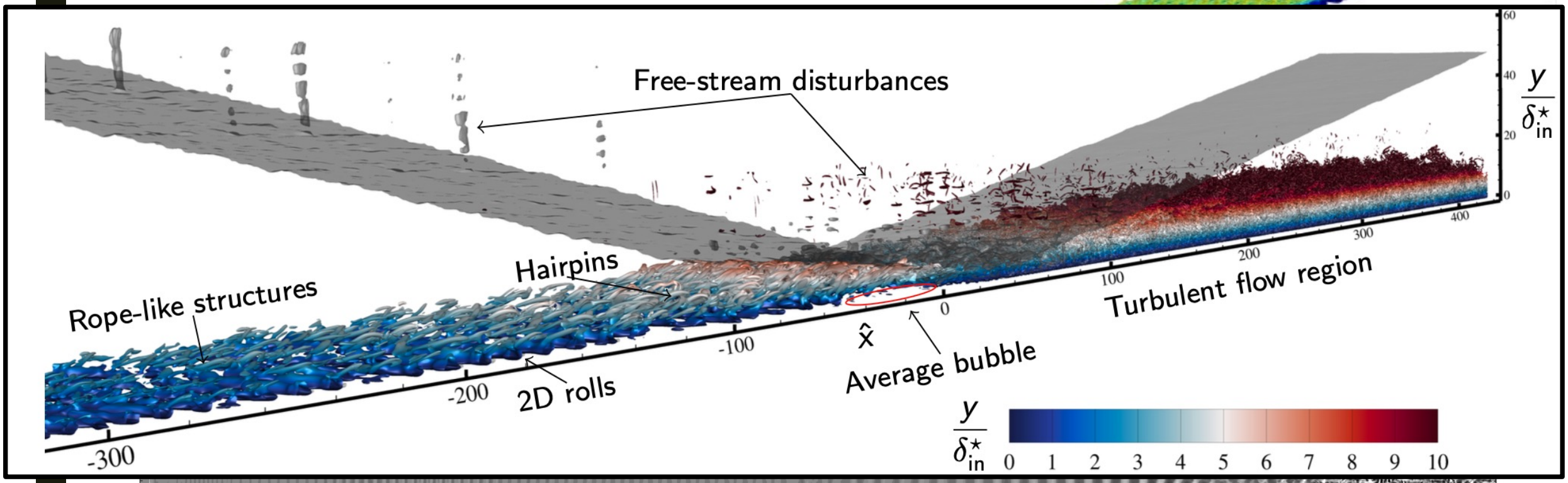


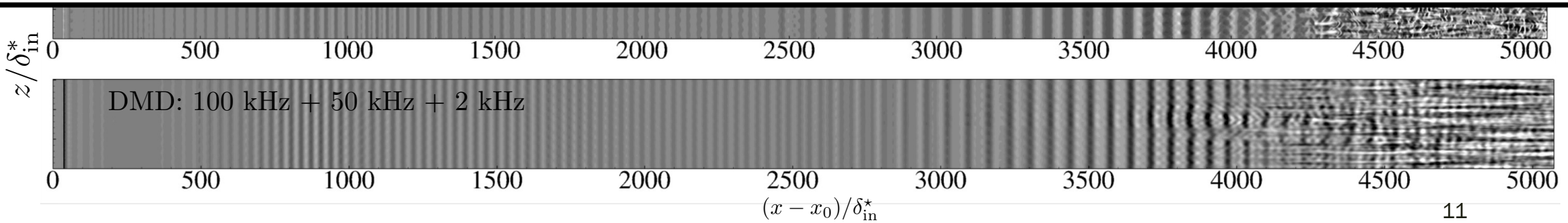
- Shock-impingement on a transitional boundary layer
- High thermal non-equilibrium
- Extreme vibrational excitation at the shock impingement



Second-mode transition

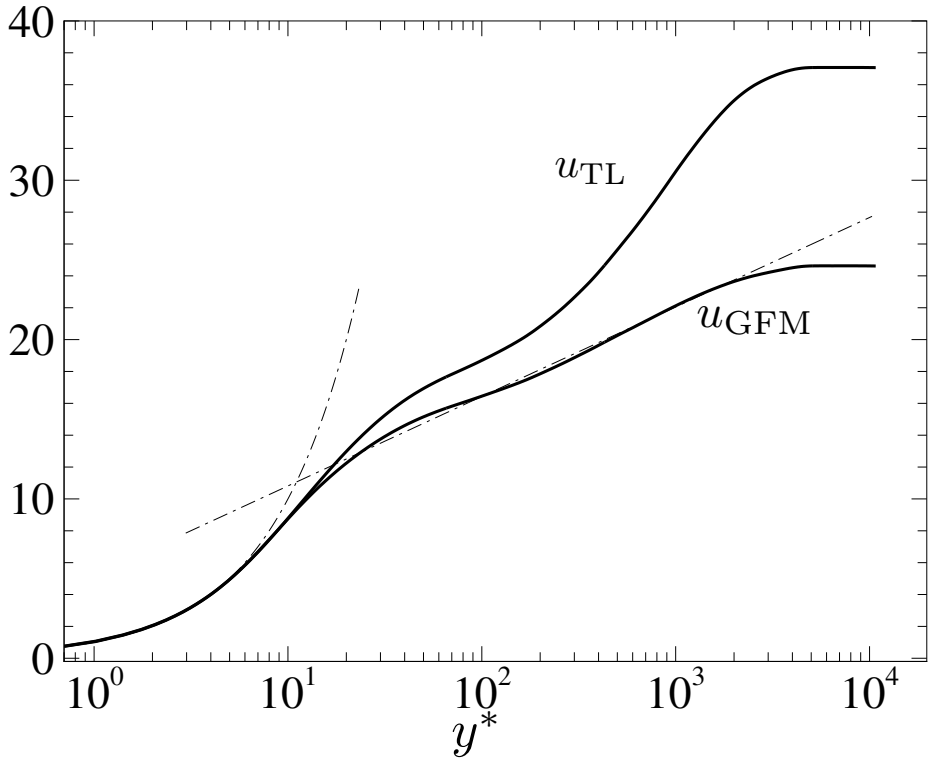
CNE*Adia*

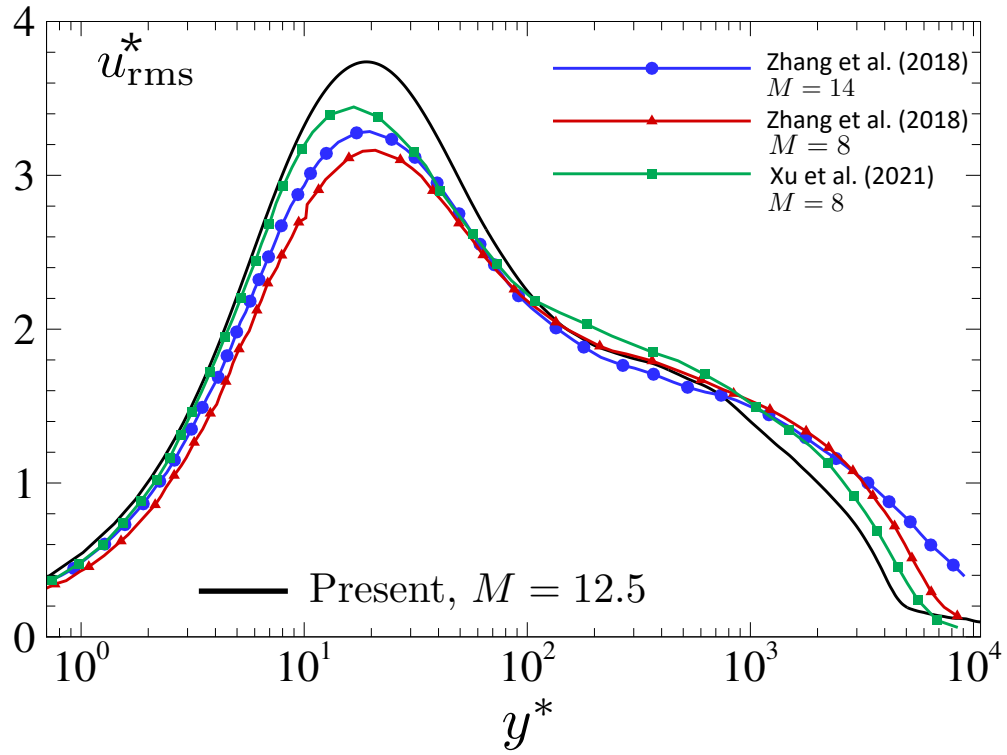




Turbulence dynamics

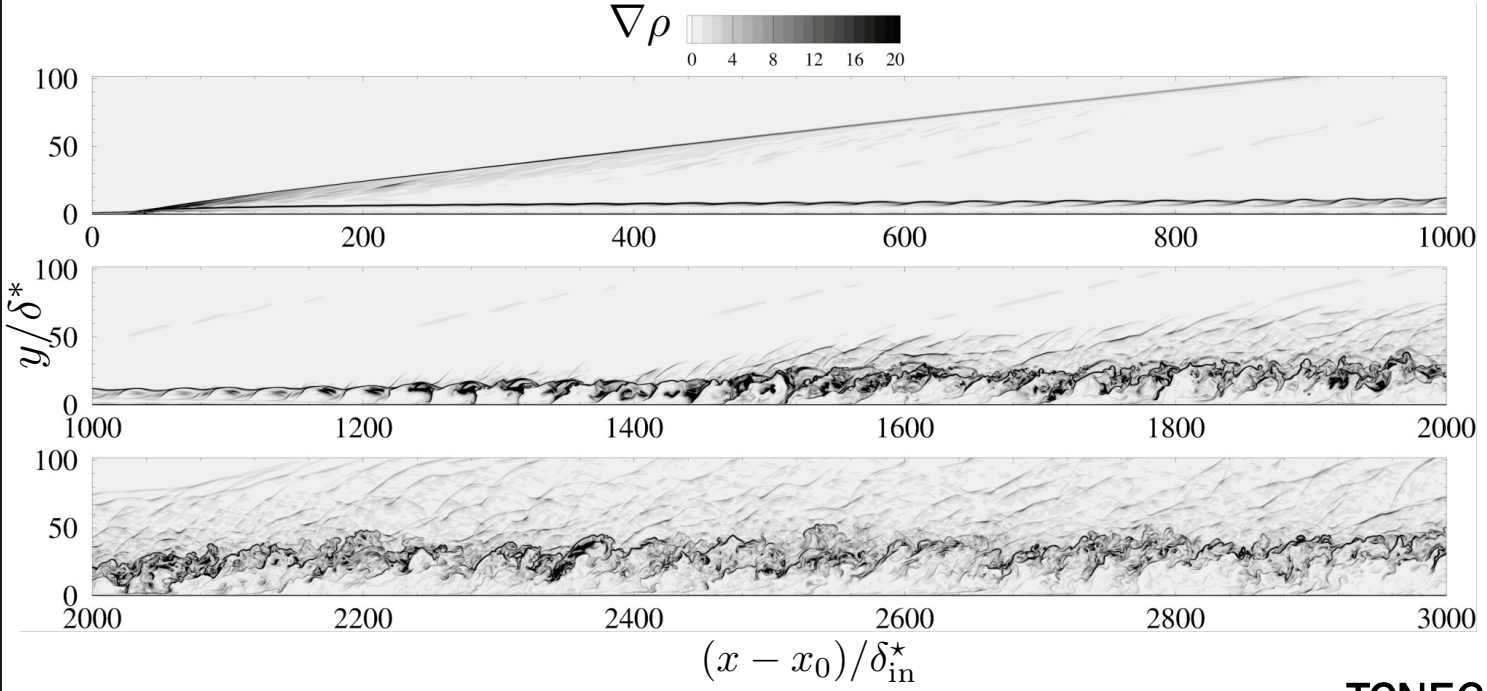
TCNE*Cool*

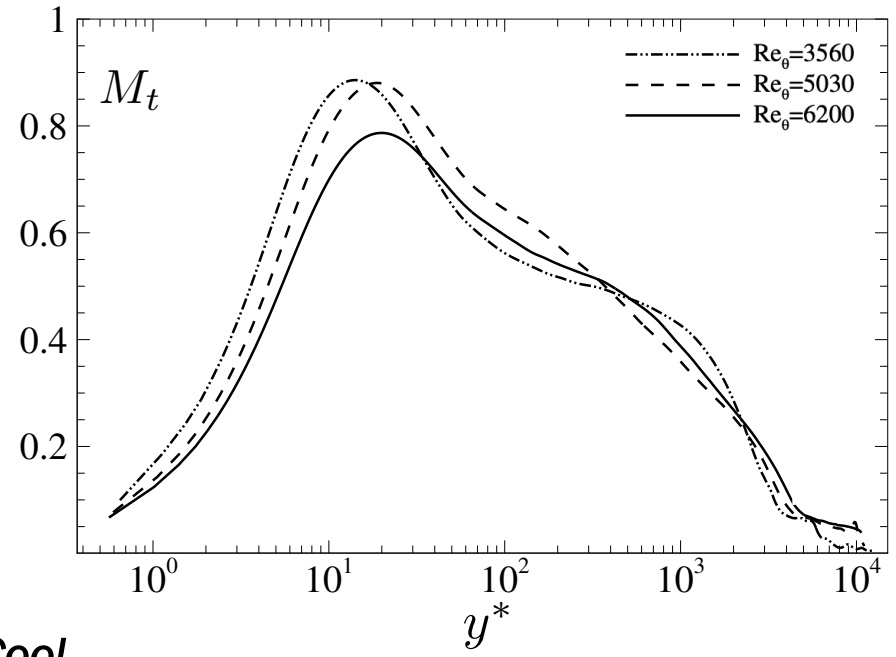




- Existing compressible scaling can be used, as long as Morkovin's hypothesis stands
- Qualitative similar behavior to cryogenic hypersonic boundary layers

Compressibility effects

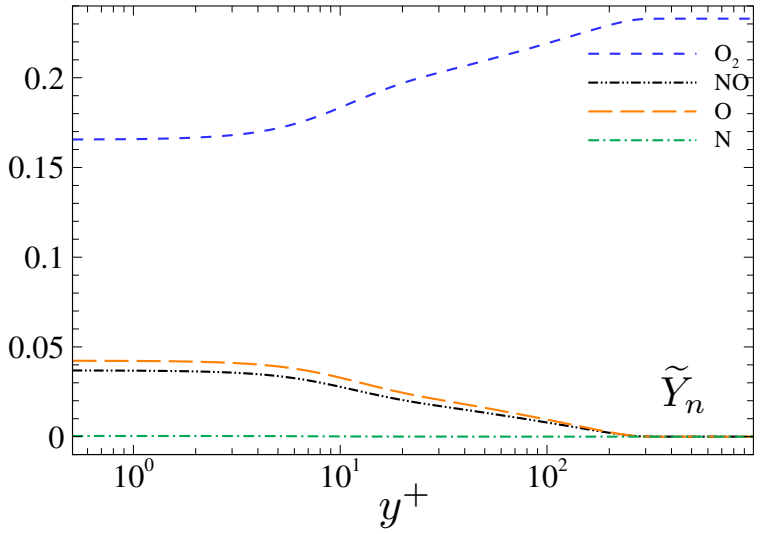


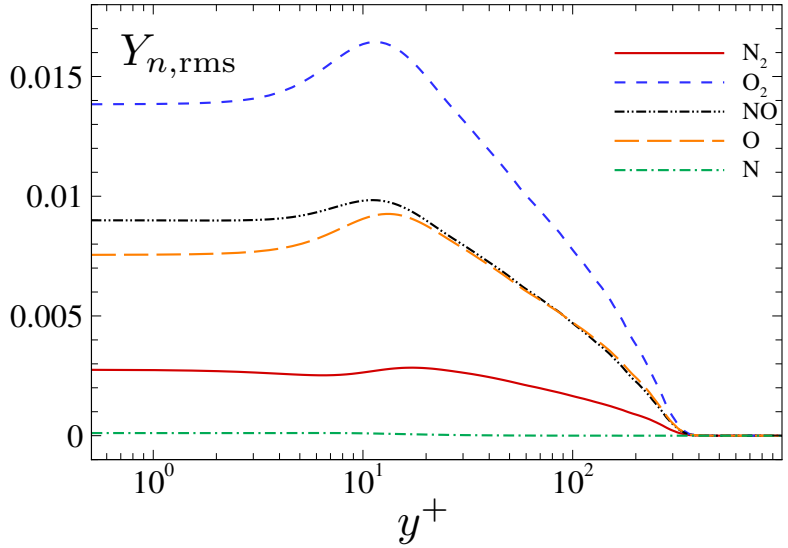


TCNE*Cool*

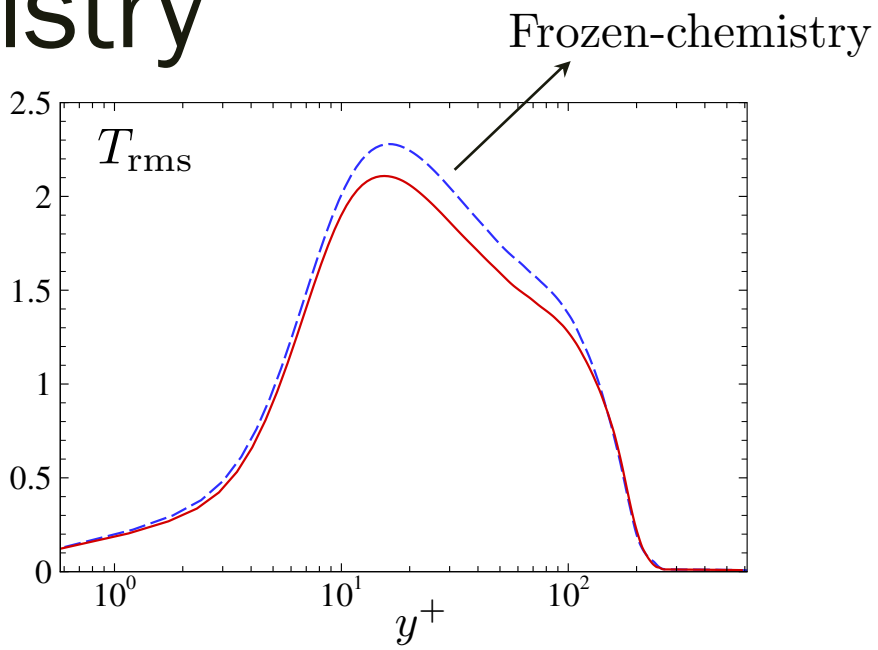
- High-turbulent Mach number; strong compressibility effects, mainly at boundary layer edge

Turbulence & chemistry



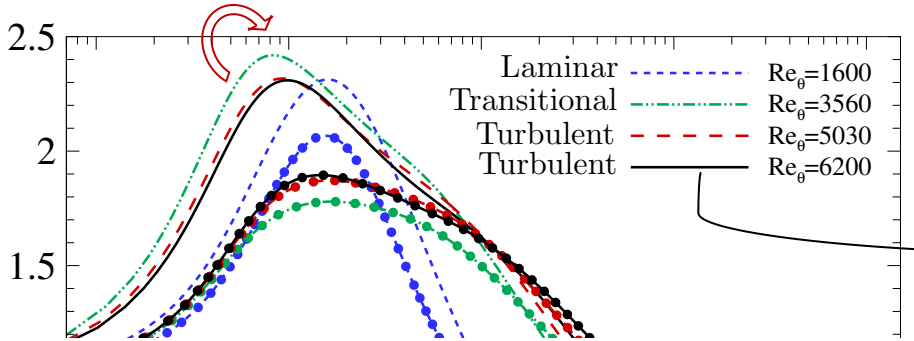


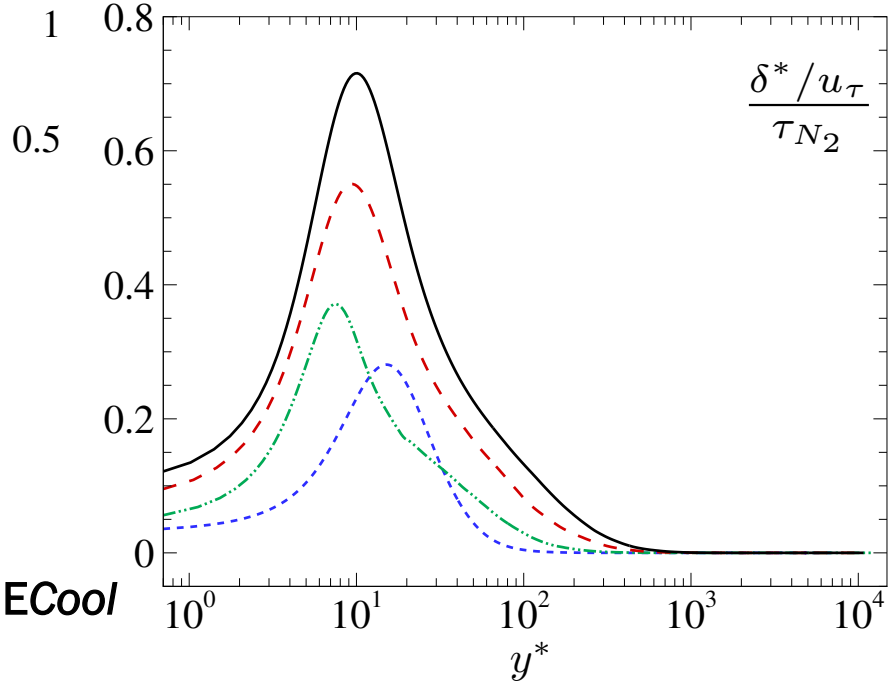
CNE*Adia*



- Relatively small chemical dissociation. Decoupling of flow and chemical time scales (small Damkholer numbers)
- Peak of species fluctuations matches peak of temperature fluctuations
- Comparison against a frozen chemistry assumption (i.e., no chemical activity) reveals that temperature fluctuations decrease due to the endothermic nature of the reactions

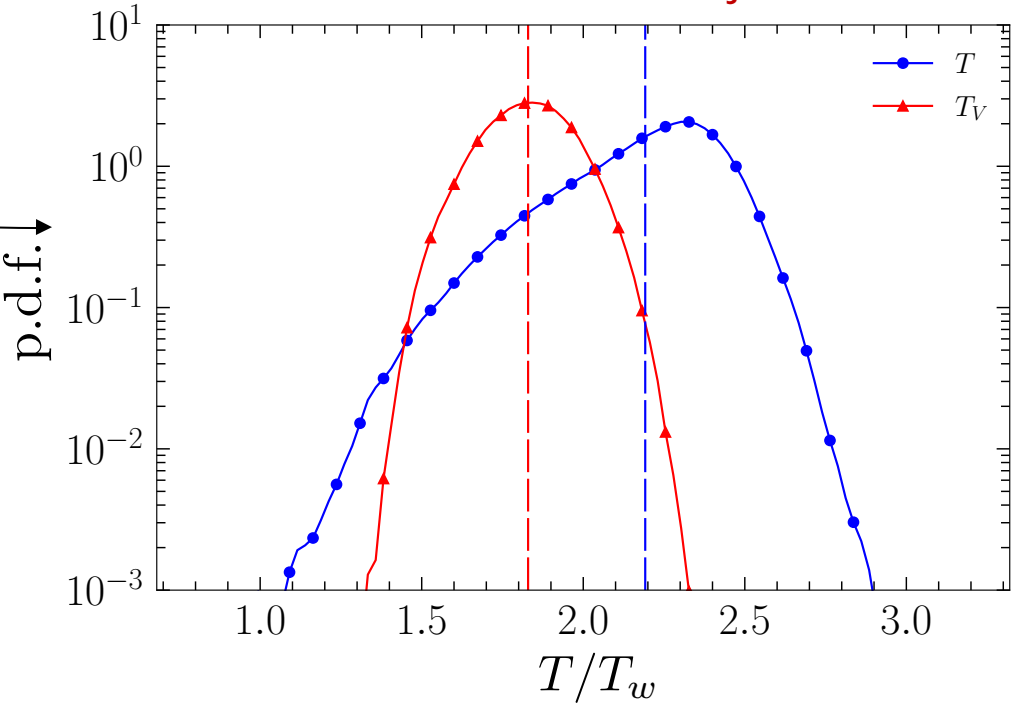
Turbulence & thermal excitation





TCNE*Cool*

Ejections



- Largest thermal non-equilibrium in the buffer layer
- Large temperatures difference in the fully turbulent region, due to sweeps and ejections events
- Main responsible for thermal non-equilibrium is molecular nitrogen (Damkholer number of order 1)

Considerations on closure modeling (I)

$$\overline{\rho}\left(\widetilde{u_i u_j} - \widetilde{u}_i \widetilde{u}_j\right) = \tau_{ij}^{\mathrm{SGS}} - \frac{1}{3}\tau_{kk}^{\mathrm{SGS}} = -2\mu_{\mathrm{SGS}}\left(\widetilde{S}_{ij} - \frac{1}{3}\widetilde{S}_{kk}\delta_{ij}\right),$$

$$\overline{\rho}\left(\widetilde{hu_j} - \widetilde{h}\widetilde{u_j}\right) = -\frac{\mu_{\mathrm{SGS}}}{Pr_{\mathrm{SGS}}}\frac{\partial \widetilde{h}}{\partial x_j}$$

$$\overline{\rho}\left(\widetilde{Y_n u_j} - \widetilde{Y}_n \widetilde{u}_j\right) = -\frac{\mu_{\mathrm{SGS}}}{Sc_{\mathrm{n,SGS}}}\frac{\partial \widetilde{Y}_n}{\partial x_j}$$

$$\overline{\rho}\left(\widetilde{e_V u_j} - \widetilde{e_V}\widetilde{u}_j\right) = -\frac{\mu_{\mathrm{SGS}}}{Pr_{\mathrm{SGS},V}}\frac{\partial \widetilde{e_V}}{\partial x_j}$$

$$\tau_{ij}^{\mathrm{SGS}} - \frac{1}{3}\tau_{kk}^{\mathrm{SGS}} = -2\mu_{\mathrm{SGS}}\left(\widetilde{S}_{ij} - \frac{1}{3}\widetilde{S}_{kk}\delta_{ij}\right)$$

$$\tau_{kk}^{\mathrm{SGS}} = 2C_I\overline{\rho}\Delta^2|\tilde{S}|^2$$

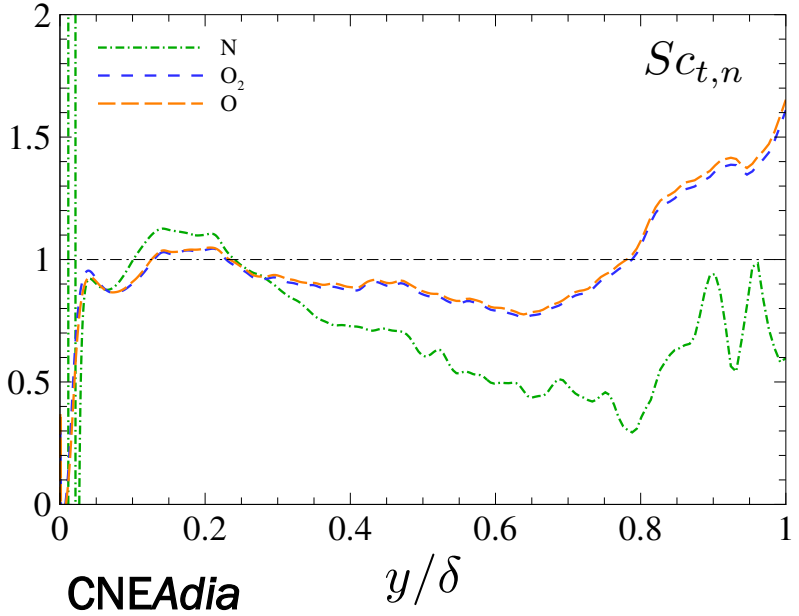
ies

$-\widetilde{u}_j\widetilde{e}_{\mathrm{V}})]$

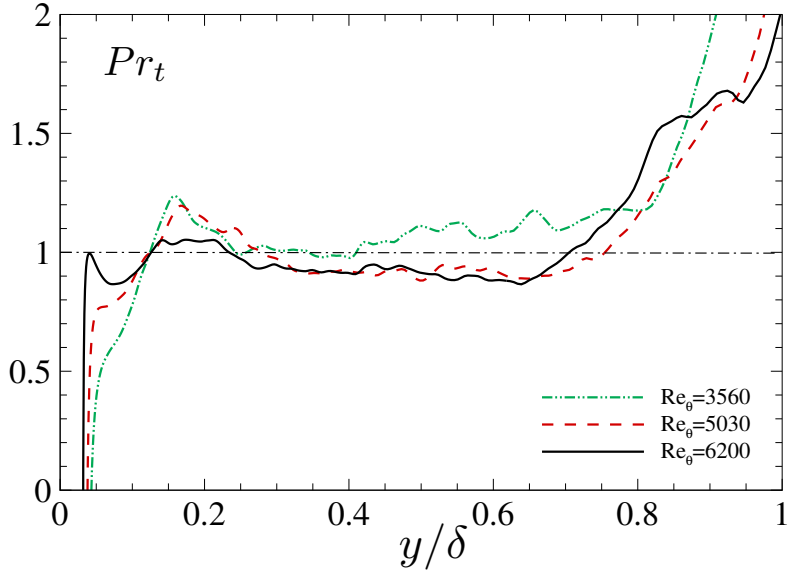
Vibrational energy

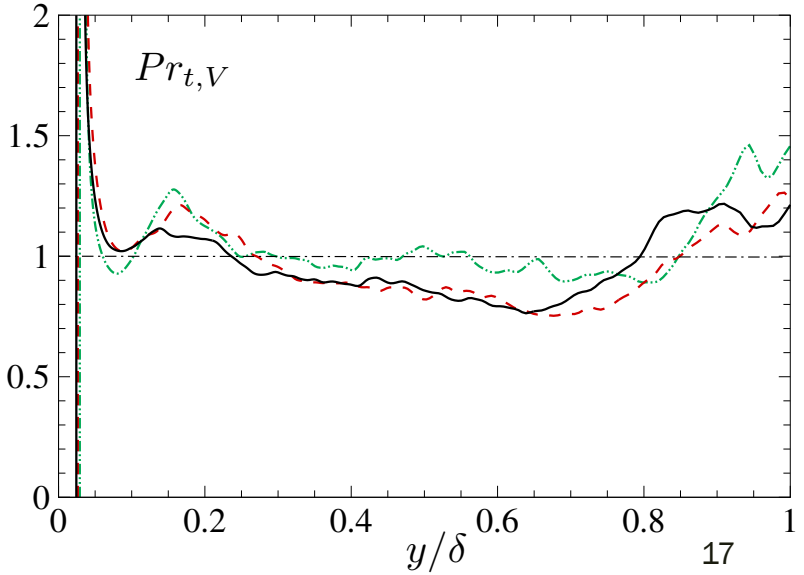
Considerations on closure modeling (II) TCNE*Cool*

$$\frac{\overline{\rho u'' v''}\,\partial \widetilde{f}/\partial y}{\overline{\rho v'' f''}\,\partial \widetilde{u}/\partial y}$$



CNE*Adia*

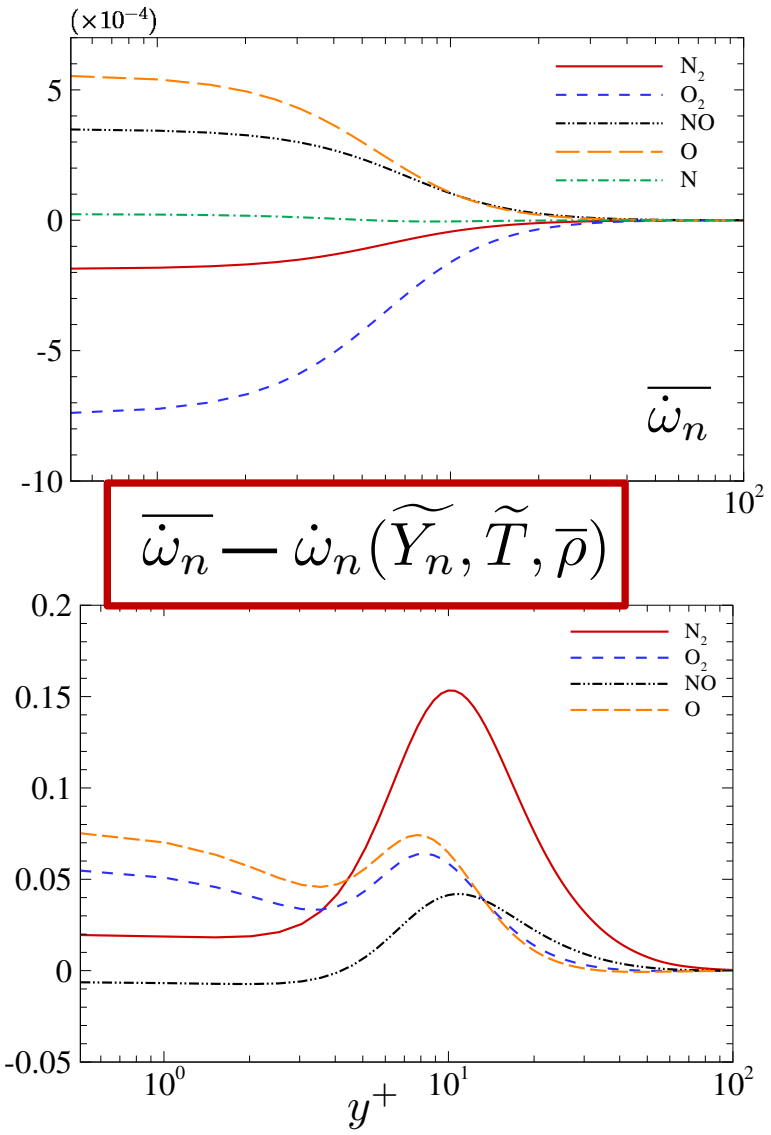




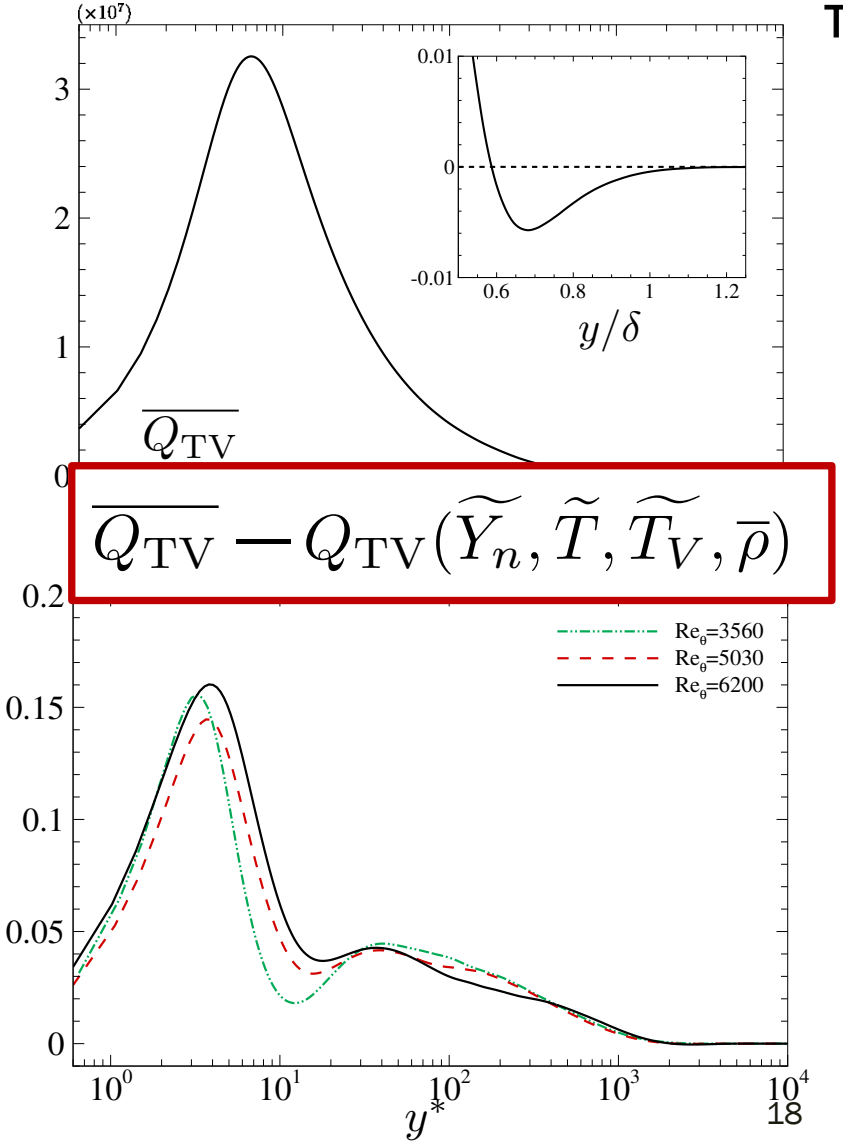
- Gradient assumption may be used, but with non-constant turbulent Prandtl number and turbulent Schmidt number
- Vibrational turbulent heat flux can be modeled by means of a vibrational turbulent Prandtl number

Considerations on closure modeling (III)

CNE*Adia*

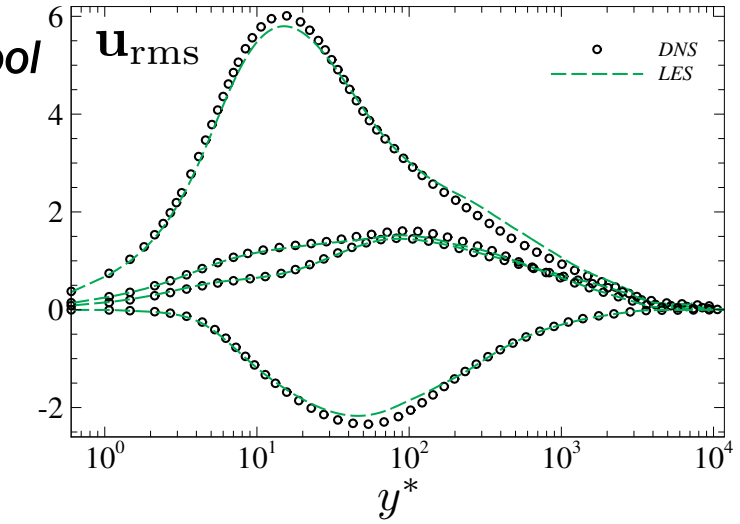


TCNE*Cool*



Tentative LES

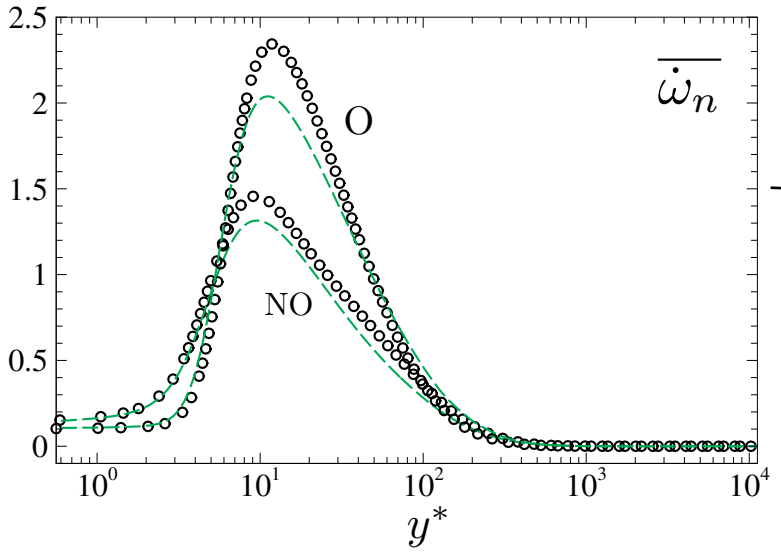
TCNE*Cool*

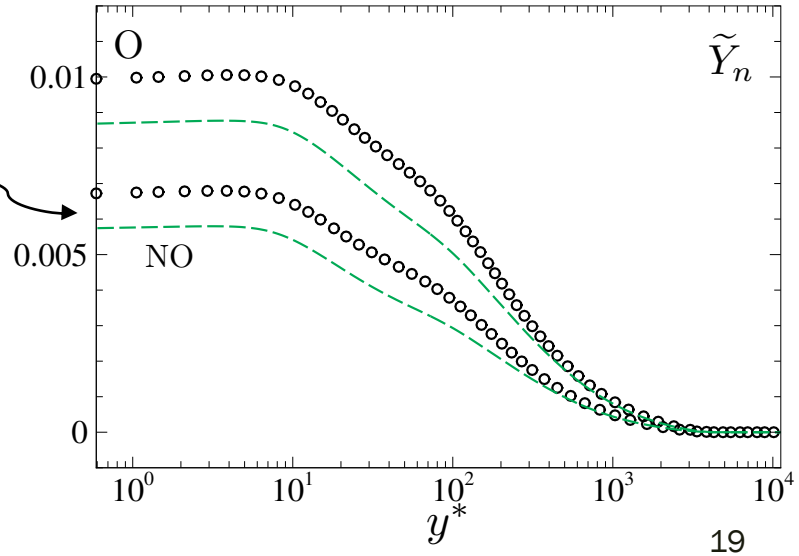


- Good-quality wall-resolved LES, but….
- … we have to do better for turbulence-chemistry interaction!

Approximation!!

$$\overline{\dot{\omega}_n} = \dot{\omega}_n(\widetilde{Y}_n, \widetilde{T}, \overline{\rho})$$





Conclusive remarks

- Compressible wall-bounded turbulence of hypersonic gases with high-temperature effects is qualitatively similar to configurations under cryogenic conditions
- The main effects of CNE being the reduction of internal energy
- CNE is reduced by turbulent mixing. TNE is tightly coupled with turbulence; the former occurs and persists because of sweep and ejection events
- Strong pressure gradients in (i.e., SWBLI configurations) further promote thermal out-of-equilibrium
- For both CNE and TCNE, unclosed source terms may be non-negligible. Attention must be paid to the development of turbulence models and scaling in the context of high-enthalpy flows

- Work in progress:
  Collaboration with Stanford. Turbulence-chemistry interaction modeling for LES
  Collaboration with Prof. Mario Di Renzo. Turbulent scaling for finite-rate chemistry

- Passiatore D., Sciacovelli L., Cinnella P., Pascazio G. -- **Evaluation of a high-order central-difference solver for highly compressible flows out of thermochemical equilibrium** , Submitted to Computers and Fluids, (2023)
- Passiatore D., Sciacovelli L., Cinnella P., Pascazio G. -- Shock impingement on a transitional hypersonic high-enthalpy boundary layer, Physical Review Fluids, 8, 044601, (2023)
- Passiatore D., Sciacovelli L., Cinnella P., Pascazio G. -- **Thermochemical nonequilibrium effects in turbulent hypersonic boundary layers, Journal of Fluid Mechanics**, 941, A21, (2022)
- Sciacovelli L., Passiatore D., Cinnella P., Pascazio G. -- **Assessment of a high-order shock-capturing central-difference scheme for hypersonic turbulent flow simulations**, Computers and Fluids, 230, 105134, (2021)
- Passiatore D., Sciacovelli L., Cinnella P., Pascazio G. -- **Finite-rate chemistry effects in hypersonic boundary layers: a direct numerical simulation study**, Physical Review Fluids, 6.5, 054604, (2021)
- Cannici A., Passiatore D., Sciacovelli L., Cinnella P. -- **A priori tests of turbulence models for compressible flows**, 56 3AF International Conference on Applied Aerodynamics (2023), France
- Passiatore D., Sciacovelli L., Cinnella P., Pascazio G. -- **Numerical investigation of hypersonic turbulent boundary layers with high-temperature effects** , 33 Congress of he international council of he aeronautical sciences (2022)

Backup Slides

Hypersonic regime:
Conversion of kinetic energy into internal energy $\Longrightarrow$ high-temperature effects

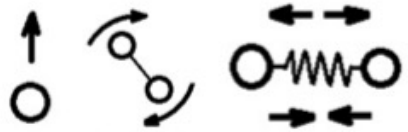
Low temperature: $e = e_{tr} + e_{rot} + (e_{vib} + e_{el})$



If the temperature increases:

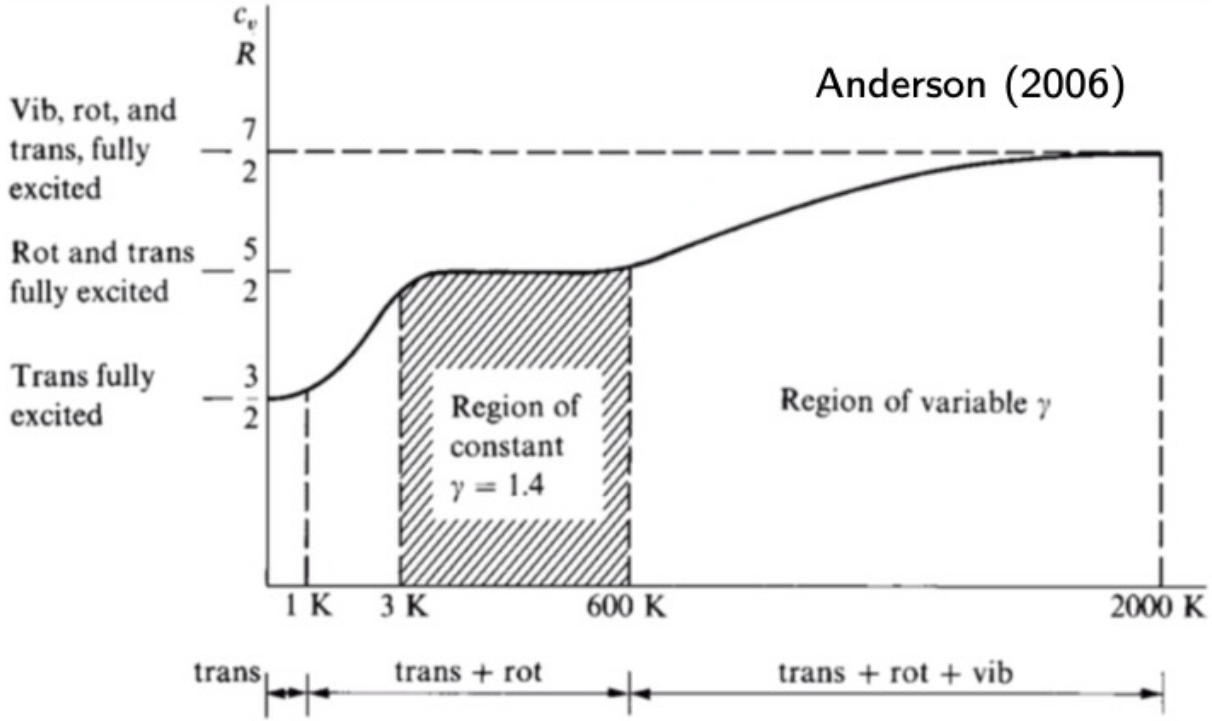
- $T > 600\,\mathrm{K}$: Vibrational excitation

$$e = e_{tr} + e_{rot} + e_{vib} + (e_{el})$$



- $T > 2000\,\mathrm{K}$: Chemical reactions
  - Dissociation of O_2 and N_2
  - Recombination reactions; formation of NO

- $T > 9000\,\mathrm{K}$: Ionization



- Different characteristic times for each process

$$\tau_{tr} \neq \tau_{rot} \neq \tau_{vib} \neq \tau_{diss} \neq \tau_{el}$$

Chemical and vibrational relaxation times must be compared to flow time scales:

- $\tau_{flow}/\tau \gg 1$: **Equilibrium**
  - Equilibrium composition instantly reached
  - Vibrational relaxation extremely fast
- $\tau_{flow}/\tau \ll 1$: **Frozen**
  - Species mass fractions do not change
  - Vibrational energy is constant

What happens when $\tau_{flow}/\tau \approx 1$?

$$e = e_{tr} + e_{rot} + e_{vib} \quad (+e_{el}(T))$$

$$e = \frac{3}{2}RT + RT + \frac{\theta_V RT}{e^{\theta_V/T}-1} \quad (+e_{el}(T))$$

$$e = \frac{3}{2}RT_{tr} + RT_{rot} + \frac{\theta_V RT_{vib}}{e^{\theta_V/T_{vib}}-1} (+e_{el}(T_{el}))$$

$$T_{tr} = T_{rot} \neq T_{vib} (\neq T_{el})$$

Mixture: N_2, O_2, NO, O, N. (M, generic third body)

R1: $N_2 + M \Longleftrightarrow 2N + M$

R2: $O_2 + M \Longleftrightarrow 2O + M$

R3: $NO + M \Longleftrightarrow N + O + M$

R4: $N_2 + O \Longleftrightarrow NO + N$

R5: $NO + O \Longleftrightarrow N + O_2$

- Finite relaxation times: **T**hermal **N**on-**E**quilibrium
- Finite reaction rates: **C**hemical **N**on-**E**quilibrium
- CNE accounts for TNE by using $T_a \rightarrow$ **TCNE**
  $T_a = T^q T_V^{1-q}$, $q \in [0.7, 0.5]$ (Park's 2T model)

$$\frac{\partial \rho}{\partial t} + \frac{\partial \rho u_j}{\partial x_j} = 0$$

$$\frac{\partial \rho u_i}{\partial t} + \frac{\partial \left(\rho u_i u_j + p\delta_{ij}\right)}{\partial x_j} = \frac{\partial \tau_{ij}}{\partial x_j}$$

$$\frac{\partial \rho E}{\partial t} + \frac{\partial \left[\left(\rho E + p\right) u_j\right]}{\partial x_j} = \frac{\partial (u_i \tau_{ij} - q_j - q_{V,j})}{\partial x_j} - \frac{\partial}{\partial x_j}\left[\sum_{n=1}^{\mathrm{NS}} \rho_n u_{n,j}^D h_n\right]$$

$$\frac{\partial \rho_n}{\partial t} + \frac{\partial \left(\rho_n u_j\right)}{\partial x_j} = -\frac{\partial \rho_n u_{n,j}^D}{\partial x_j} + \dot{\omega}_n \quad (n=1,\ldots,\mathrm{NS}-1)$$

$$\frac{\partial \rho e_V}{\partial t} + \frac{\partial \left(\rho e_V u_j\right)}{\partial x_j} = -\frac{\partial}{\partial x_j}\left(q_{V,j} + \sum_{m=1}^{\mathrm{NM}} \rho_n u_{m,j}^D e_{V,m}\right) + \sum_{m=1}^{\mathrm{NM}} \left(Q_{\mathrm{TV},m} + Q_{\mathrm{chem},m}\right)$$

		N_2	O_2	NO	O	N
$\mathcal{M}$	[g/mol]	28	32	30	16	14
θ_V	[K]	3393	2270	2739	-	-
h_f^0	[kJ/mol]	0	0	91.27	249.2	472.7
T_c	[K]	126.2	154.8	180		
p_c	[MPa]	3.39	5.08	6.48		

- **Thermally perfect gas model (TRV formulation)**:

$$p = \sum_{n=1}^{\mathrm{NS}} p_n = \rho T \sum_{n=1}^{\mathrm{NS}} \frac{\mathcal{R} Y_n}{\mathcal{M}_n} = T \sum_{n=1}^{\mathrm{NS}} \rho_n R_n$$

$$h_n = h_{f,n}^0 + \int_{T_{\mathrm{ref}}}^{T} \left(c_{p,n}^{\mathrm{tr}} + c_{p,n}^{\mathrm{rot}}\right) \mathrm{d}T' + e_n^{\mathrm{vib}}(T_V)$$

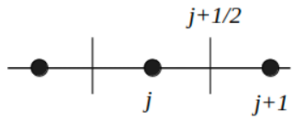
- **Viscosity and thermal conductivities**:
  Blottner curve fitting
  Eucken's correction
  Wilke's mixing rules

- **Mass diffusion**:
  Gupta curve fitting
  Hirschfelder approximation
  Mass corrector term

- **Thermochemical models**:
  Park's 2T model

Artificial dissipation + Shock capturing approaches

$$\frac{\partial w}{\partial t}+\frac{\partial f(w)}{\partial x}=0 \quad \Longrightarrow \quad \left.\frac{\partial w}{\partial t}\right|_j+\frac{(\delta \mathcal{F})_j}{\delta x}=0 \quad \text{with} \quad \begin{aligned}(\delta \bullet)_{j+\frac{1}{2}} &= (\bullet)_{j+1}-(\bullet)_j \\ (\mu \bullet)_{j+\frac{1}{2}} &= \frac{1}{2}\left[(\bullet)_{j+1}+(\bullet)_j\right]\end{aligned}$$



↪ Upwind first-order scheme: $\mathcal{F}_{j+\frac{1}{2}}=\mathcal{H}_{j+\frac{1}{2}}-\mathcal{D}_{j+\frac{1}{2}}=\frac{f_{j+1}+f_j}{2}-\frac{1}{2}Q_{j+\frac{1}{2}}(w_{j+1}-w_j)=(\mu f)_{j+\frac{1}{2}}-\frac{1}{2}(Q\delta w)_{j+\frac{1}{2}}$

↪ High-order achieved by means of **recursive correction** of the truncation error:

$$\begin{aligned}
&&\frac{\partial f}{\partial x}&\approx\frac{\delta\mu f_j}{\Delta x} && \Longrightarrow && \epsilon&=+\frac{\Delta x^2}{6}\frac{\partial^3 f}{\partial x^3}+\mathcal{O}(\Delta x^4)\\
\frac{\partial^3 f}{\partial x^3}=\frac{\delta^3\mu f}{\Delta x^3}+\mathcal{O}(\Delta x^4) && \Longrightarrow && \frac{\partial f}{\partial x}&\approx\left[I-\frac{\delta^2}{6}\right]\frac{\delta\mu f_j}{\Delta x} && \Longrightarrow && \epsilon&=-\frac{\Delta x^4}{30}\frac{\partial^5 f}{\partial x^5}+\mathcal{O}(\Delta x^6)\\
\frac{\partial^5 f}{\partial x^5}=\frac{\delta^5\mu f}{\Delta x^5}+\mathcal{O}(\Delta x^6) && \Longrightarrow && \frac{\partial f}{\partial x}&\approx\left[I-\frac{\delta^2}{6}+\frac{\delta^4}{30}\right]\frac{\delta\mu f_j}{\Delta x} && \Longrightarrow && \epsilon&=+\frac{\Delta x^6}{140}\frac{\partial^7 f}{\partial x^7}+\mathcal{O}(\Delta x^8) \quad \ldots
\end{aligned}$$

- Centered scheme
- High-order dissipation
- Low-order shock capturing

$$
\begin{aligned}
\mathcal{F}_{j+\frac{1}{2}} &= \mathcal{H}_{j+\frac{1}{2}} - \mathcal{D}_{j+\frac{1}{2}} \\
&= \left[\mu f - \frac{Q}{2} \delta w \right]_{j+\frac{1}{2}} \\
&= \left[\left(I - \frac{\delta^2}{6} \right) \mu f + \rho(A) \left(\varepsilon_2 \delta w - \varepsilon_4 \delta^3 w \right) \right]_{j+\frac{1}{2}} \\
&= \left[\left(I - \frac{\delta^2}{6} + \frac{\delta^4}{30} \right) \mu f - \rho(A) \left(\varepsilon_2 \delta w - \varepsilon_6 \delta^5 w \right) \right]_{j+\frac{1}{2}} \\
&= \left[\left(I - \frac{\delta^2}{6} + \frac{\delta^4}{30} - \frac{\delta^6}{140} \right) \mu f + \rho(A) \left(\varepsilon_2 \delta w - \varepsilon_8 \delta^7 w \right) \right]_{j+\frac{1}{2}} \\
&= \left[\left(I - \frac{\delta^2}{6} + \frac{\delta^4}{30} - \frac{\delta^6}{140} + \frac{\delta^8}{630} \right) \mu f - \rho(A) \left(\varepsilon_2 \delta w - \varepsilon_{10} \delta^9 w \right) \right]_{j+\frac{1}{2}}
\end{aligned}
$$

$$
\begin{aligned}
\varepsilon_2 &= k_2 \max(\varphi_j, \varphi_{j+1}) \\
\varepsilon_4 &= \max(0, k_4 - \varepsilon_2) \\
\varepsilon_6 &= \max(0, k_6 - \frac{1}{5}\varepsilon_2) \\
\varepsilon_8 &= \max(0, k_8 - \frac{3}{70}\varepsilon_2) \\
\varepsilon_{10} &= \max(0, k_{10} - \frac{1}{105}\varepsilon_2)
\end{aligned}
$$

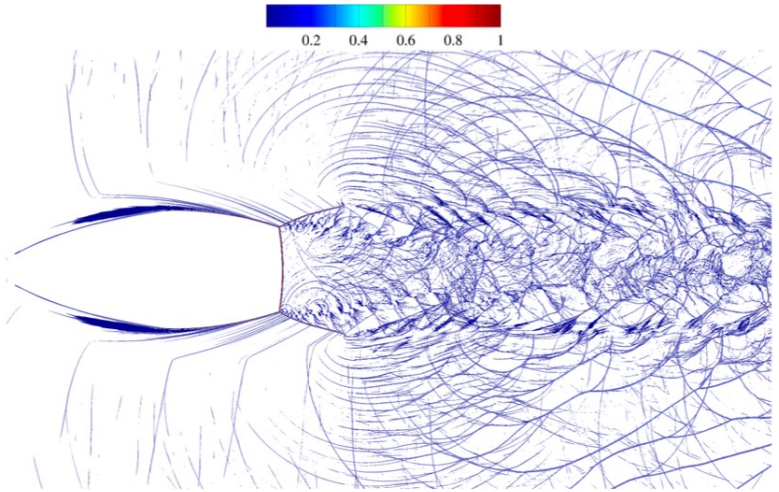
$$
\mathcal{F}_{j+\frac{1}{2}} = \left[\left(I - \sum_{p=0}^{P} a_p \delta^{2+2p} \right) \mu f - \rho(A) \left(\varepsilon_2 \delta w + \varepsilon_{2(P+2)} \delta^{2P+3} w \right) \right]_{j+\frac{1}{2}} \quad \text{with} \quad \begin{cases} \varepsilon_{2_{j+\frac{1}{2}}} = k_2 \max(\varphi_j, \varphi_{j+1}) \\ \varepsilon_{2(P+2)_{j+\frac{1}{2}}} = \max(0, k_{2(P+2)} - k_\varepsilon \varepsilon_{2_{j+\frac{1}{2}}}) \end{cases}
$$

Sciacovelli et al. - *Comput Fluids* (2021)

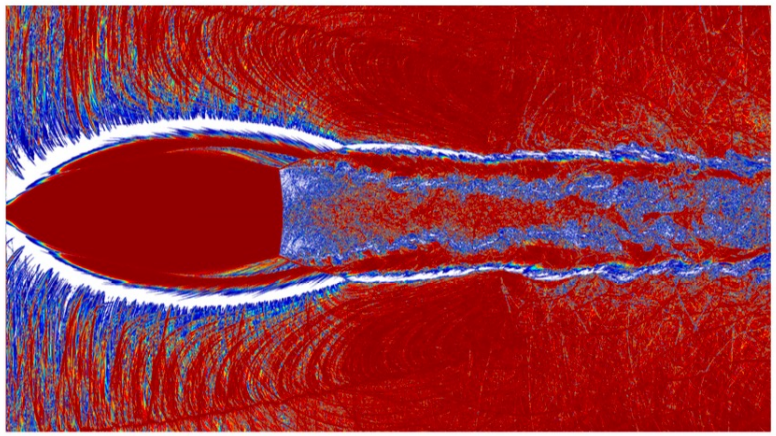
$$\varepsilon_2 = k_2 \max(\varphi_j, \varphi_{j+1})$$

$$\varphi_j = \underbrace{\frac{1}{2}\left[1 - \tanh\left(2.5 + 10\frac{\Delta x}{a}\nabla\cdot\boldsymbol{u}\right)\right]}_{\text{(I) Bhagatwala \& Lele}} \times \underbrace{\frac{(\nabla\cdot\boldsymbol{u})^2}{(\nabla\cdot\boldsymbol{u})^2 + |\nabla\times\boldsymbol{u}|^2 + \epsilon}}_{\text{(II) Ducros}} \times \underbrace{\left|\frac{p_{j+1} - 2p_j + p_{j-1}}{p_{j+1} + 2p_j + p_{j-1}}\right|}_{\text{(III) Jameson}}$$

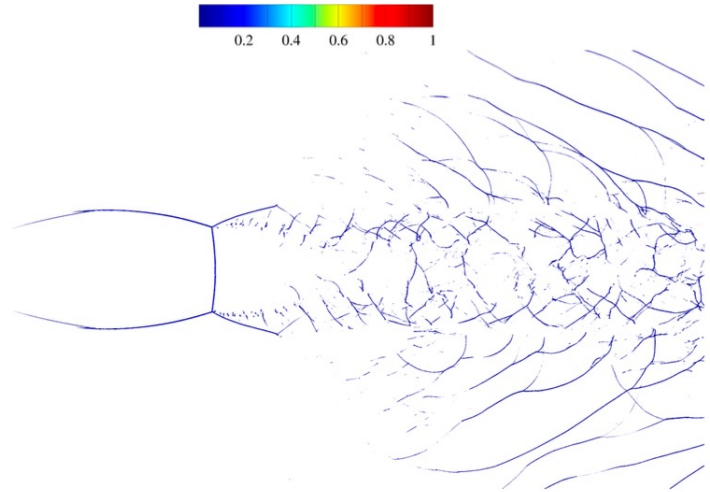
(I)



(II)



(III)



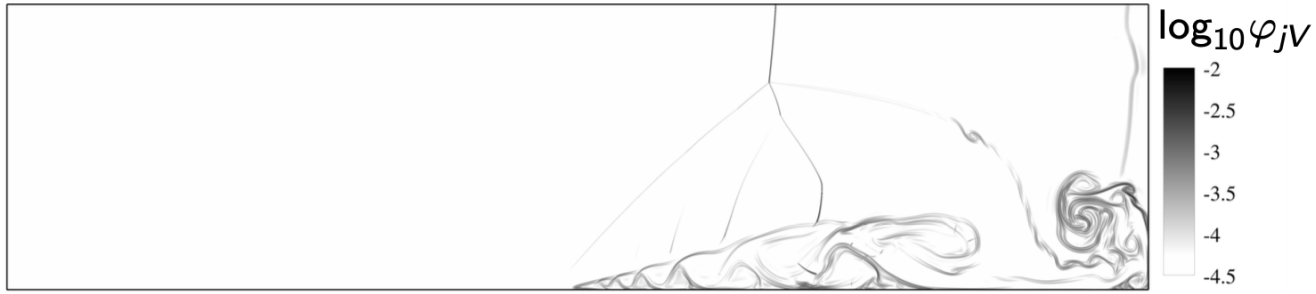
(φ)

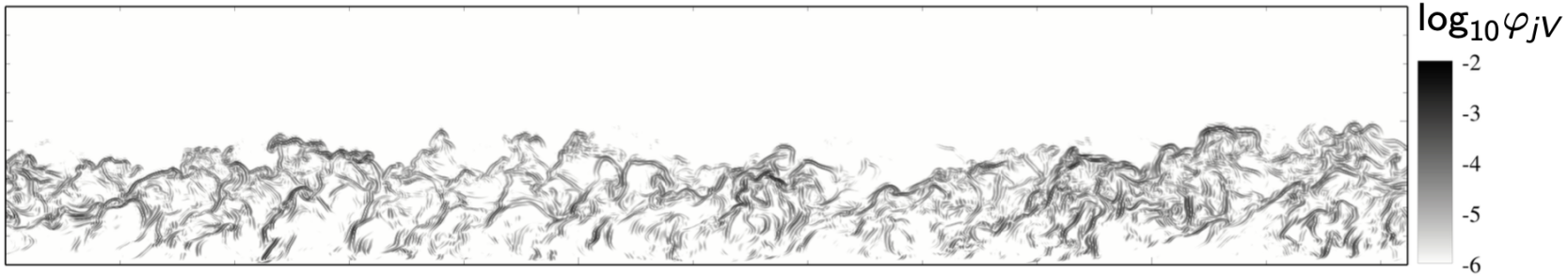


Extension to TCNE...

$$\varepsilon_2 = k_{2,V} \max(\varphi_j, \varphi_{j+1})$$

$$\varphi_{jV} = \underbrace{\left| \frac{T_{V,j+1} - 2T_{V,j} + T_{V,j-1}}{T_{V,j+1} + 2T_{V,j} + T_{V;j-1}} \right|}_{\text{Jameson modified}}$$





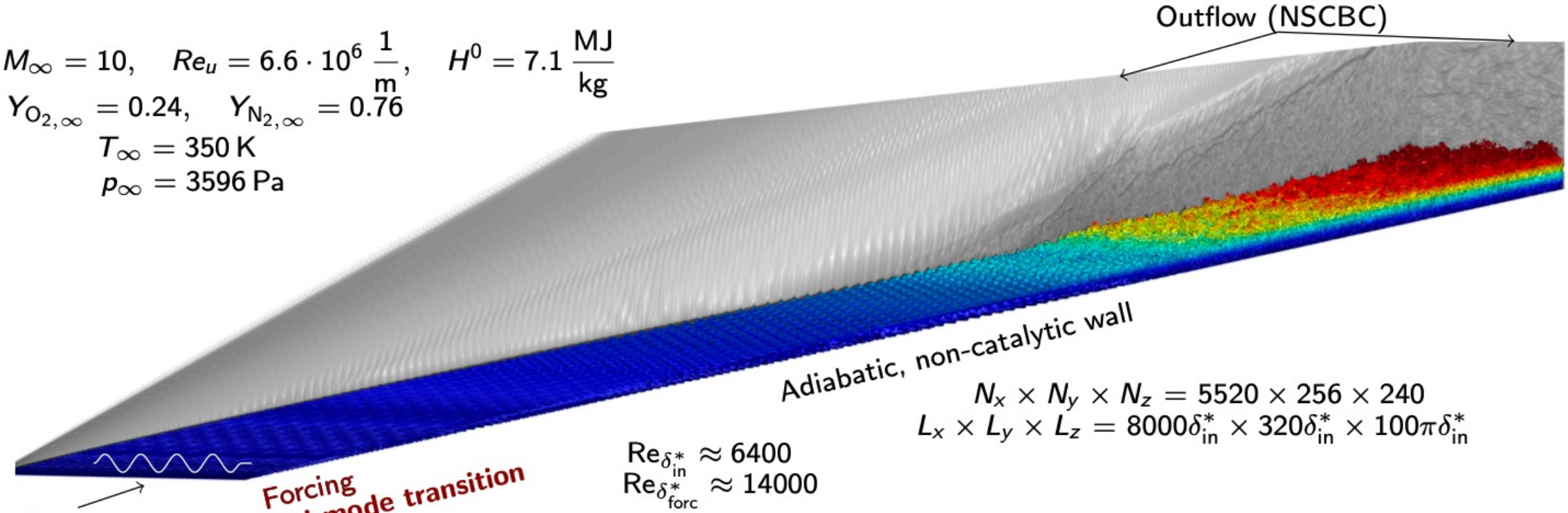
Similar to several stability studies (See works of Malik, Anderson, Marxen, Hudson, Franko..)

$M_\infty = 10, \quad Re_u = 6.6 \cdot 10^6 \frac{1}{\text{m}}, \quad H^0 = 7.1 \frac{\text{MJ}}{\text{kg}}$

$Y_{O_2,\infty} = 0.24, \quad Y_{N_2,\infty} = 0.76$

$T_\infty = 350\,\text{K}$

$p_\infty = 3596\,\text{Pa}$



$N_x \times N_y \times N_z = 5520 \times 256 \times 240$

$L_x \times L_y \times L_z = 8000\delta^*_{\text{in}} \times 320\delta^*_{\text{in}} \times 100\pi\delta^*_{\text{in}}$

$\text{Re}_{\delta^*_{\text{in}}} \approx 6400$

$\text{Re}_{\delta^*_{\text{forc}}} \approx 14000$

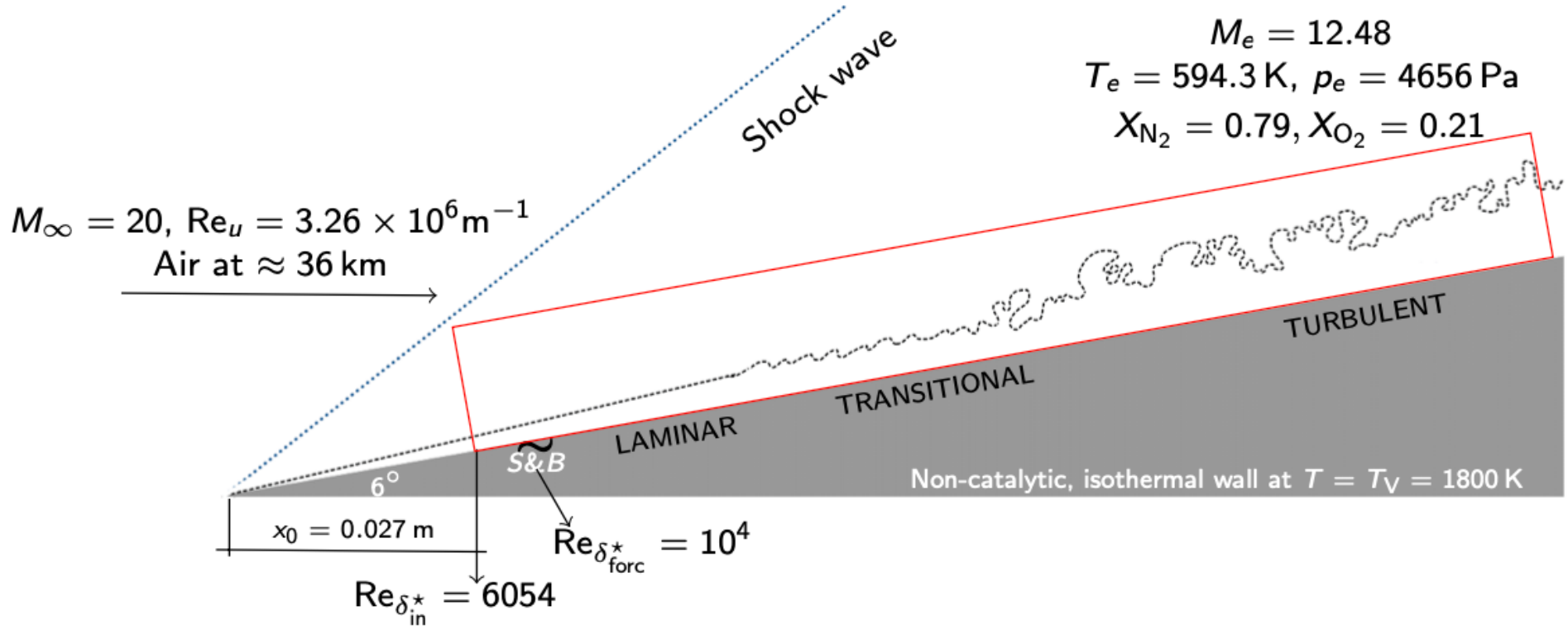
Suction & Blowing: $\frac{v_w}{u_\infty} = f(x)g(z) \sum_{m=1}^{\#\text{mode}} A_m \sin(\omega_m t + \beta_m z)$

$\omega_1 = 100\text{kHz} \times 2\pi$

$A_1 = 50 \times 10^{-3}$

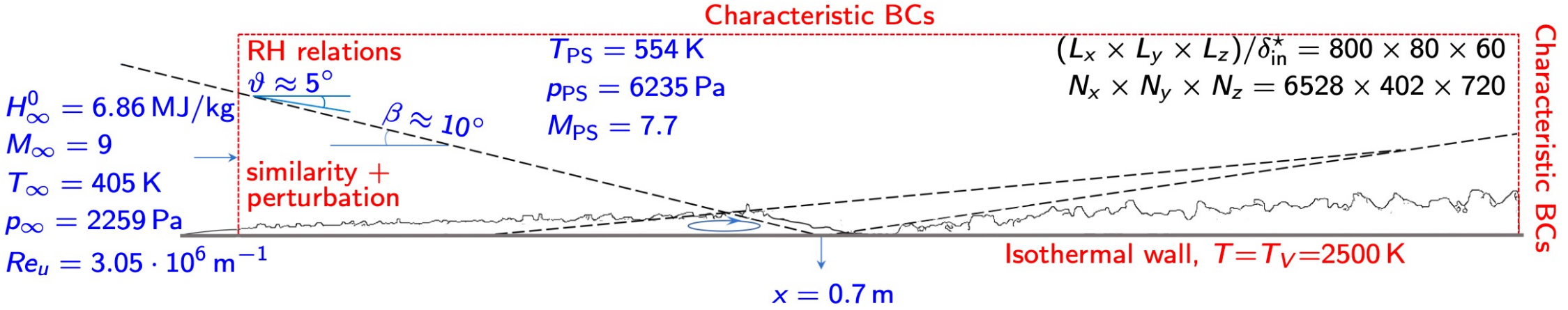
$\beta_1 = 0.2\delta^*_{\text{in}}$

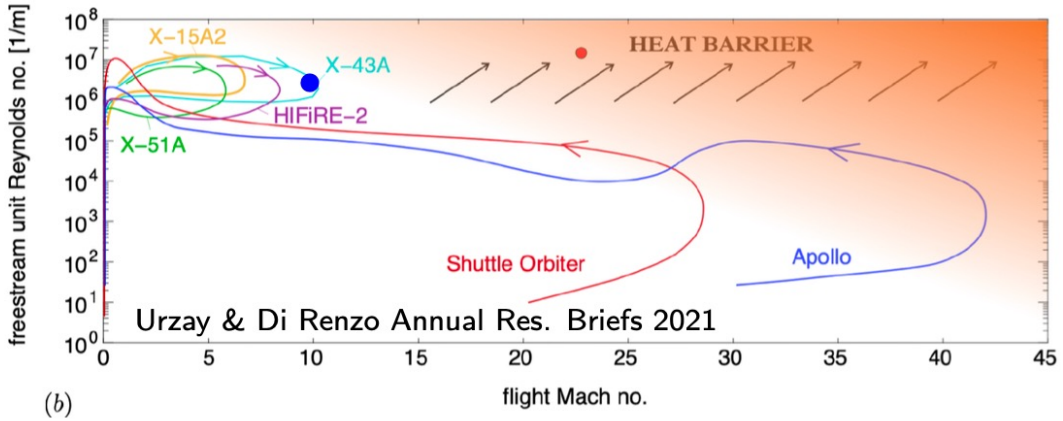
#mode	1	2	3	4	5	6	7	8	9
ω_m	ω_1	$\omega_1/2$	0	0	0	ω_1	$\omega_1/2$	ω_1	ω_1
A_m	A_1	$0.05A_1$	$0.05A_1$	$0.05A_1$	$0.05A_1$	$0.05A_1$	$0.05A_1$	$0.05A_1$	$0.05A_1$
β_m	0	0	β_1	$2\beta_1$	$3\beta_1$	$\pm\beta_1$	$\pm\beta_1$	$\pm2\beta_1$	$\pm3\beta_1$

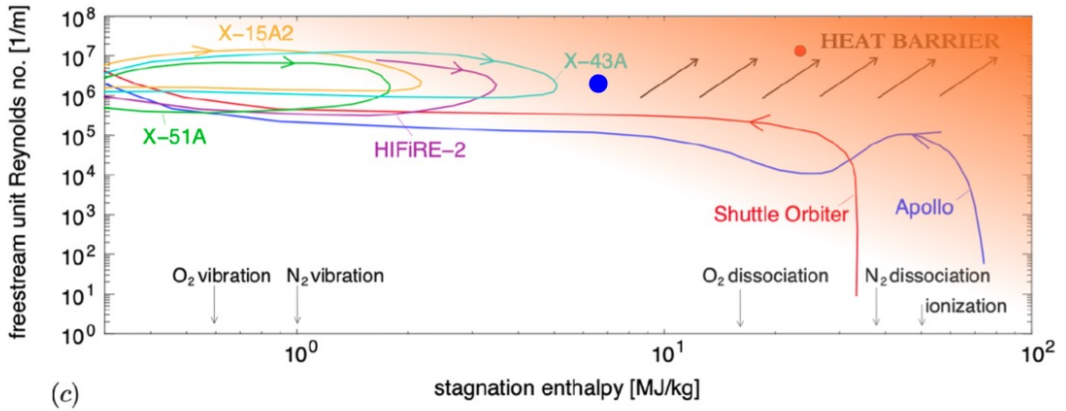


$$L_x \times L_y \times L_z = 3000\delta^*_{\mathrm{in}} \times 120\delta^*_{\mathrm{in}} \times 30\pi\delta^*_{\mathrm{in}}$$
$$N_x \times N_y \times N_z = 9660 \times 480 \times 512$$

$(x - x_0)/\delta*_{\mathrm{in}}$	744	1396	1757	2329	2900
$\mathrm{Re}_x \times 10^{-6}$	4.51	8.45	10.6	14.1	17.6
$\mathrm{Re}_{\delta*} \times 10^{-4}$	6.80	9.91	13.25	13.27	16.16
Re_θ	1600	2960	3560	5030	6200
$\mathrm{Re}_\theta^{\mathrm{inc}}$	774	1426	1716	2423	2994
Re_τ	134	670	845	983	1128
$\Delta x^+ - \Delta z^+$	4.38-2.60	10.54-6.25	8.80-5.21	7.77-4.60	7.26-4.30
$\Delta y_w^+ - \Delta y_\delta^+$	0.39-1.36	0.93-5.80	0.78-6.90	0.70-7.82	0.64-8.83







- $6°$-wedge flying at 36 km at Mach 12 (Barth *et al.* JPP 2018)
- Perturbation of self-similar profile (Sandham *et al.* JFM 2014):

$$\frac{\rho'}{\rho_\infty} = aW\left(\frac{y}{\delta^\star_{in}}\right)\sum_{j=1}^{16}\cos\left(\frac{2\pi jz}{L_z}+\Phi_j\right)\sum_{k=1}^{20}\sin\left(2\pi\widehat{f}_k\frac{u_\infty}{\delta^\star_{in}}t+\Psi_k\right)$$

- $W(y/\delta^\star_{in}) = 1-\exp[-(y/\delta^\star_{in})^3]$
- $a = 5\cdot 10^{-4}, \quad \widehat{f}_k = 0.02k$
- $\hat{x} = \dfrac{x - x_{sh}}{\delta^\star_{in}}$ used in the following